



# Strength Study of Anatomically-Similar Spongy Structures Additively Manufactured from Polymeric Materials

Łukasz Przeszlowski\*, Anna Paluch, Grzegorz Budzik, Damian Filip, Łukasz Kochmański, Mariusz Dębski

**Abstract:** The subject of the article is to investigate the potential to adjust the stiffness of 3D printed plastic implants to match bone stiffness by analyzing design parameters and mechanical properties, considering the spongy structure of the bone. The study consisted of theoretical and practical parts, including original research. In the theoretical part, the definition of implants, the materials used for their production, and the requirements they must meet were discussed, as well as 3D printing methods, with particular emphasis on the FFF method. The static compression test was also described. In the practical part, original research was conducted to verify the possibilities of adjusting the stiffness of the implants. Two 3D models of the L2 lumbar vertebra with different vertebral body thicknesses and internal lattice structures were developed based on literature dimensions. Thirty models with three different lattice densities and two wall thicknesses were printed and subjected to a static compression test. The results showed that an increase in lattice density increased the compression strength of the samples. Samples with thin walls exhibited lower compression strength compared to those with thick walls, regardless of the spongy lattice density. In each group of samples, the results were consistent, indicating good repeatability of the prepared samples. The findings suggest that appropriately selecting the lattice density and wall thickness can significantly improve the mechanical strength of bone implants, meeting the compression strength criteria for the spongy tissue of lumbar vertebrae.

**Keywords:** additive manufacturing; compression test; PLA (Polylactide) spongy structure; vertebrae

## 1 INTRODUCTION

In the medical field, the development of modern technologies such as 3D printing is opening up new perspectives in the design and manufacture of medical implants. One of the key challenges in this area is to ensure that implants are not only biocompatible, but also properly adapted to the physical and mechanical conditions of the surrounding tissues. In the context of this issue, exploring the possibility of adapting the stiffness of printed plastic implants to that of bone becomes crucial.

Properly matching the stiffness of the implant to the stiffness of the bone can help minimize the risk of injury while ensuring the stability and strength of the implant in the patient's body. In this context, it is important to understand the structure of spongy bone, which is characterized by a specific grid-like microarchitecture. Thanks to 3D printing technology, it is possible to manipulate the structural parameters of implants, including their stiffness, which opens up prospects for individualizing treatment and improving therapeutic outcomes.

The spongy structure of bone, also known as trabecular bone, is made up of tiny bone beams that form a meshwork with a large surface area. This unique structure provides exceptional strength and flexibility to bone, while allowing mechanical forces to be distributed throughout the body. In the case of medical implants, reproduction of this structure can be crucial to improving the integration of the implant into tissues and ensuring adequate stiffness and strength [2].

Compression testing of 3D printed lumbar vertebra specimens are an important part of the study. This type of mechanical test allows us to evaluate the behavior of printed implants under load, which is crucial for understanding their strength and stability under conditions similar to those in the patient's body. Modern 3D printing technology makes it possible to create implants with complex structures that can imitate the spongy structure of bone. With the help of advanced design algorithms and precise 3D printing

processes, it is possible to produce printed meshes with different geometric and mechanical parameters that are more similar to the structure of natural bone. However, it is important to pay special attention to choosing the right plastic for 3D printing implants. Plastics used in implantology have to be not only biocompatible, but also have sufficient mechanical strength and flexibility to meet the physical demands of the patient's body [8].

The purpose of this paper is to research the potential of adapting the stiffness of printed sponge structures made of selected plastic to the stiffness of spongy bone by analyzing design parameters and mechanical properties, taking into account the spongy structure of the bone and conducting compression testing of printed lumbar vertebral specimens. The research aims to develop new methods for designing and manufacturing implants to better suit individual patients' needs, and to investigate how much the stiffness of an implant can be altered with a printed lattice structure. The research aims to explore the relationship between implant design parameters, stiffness and the spongy structure of bone.

The research section presents the methodology for creating 3D models of the L2 lumbar vertebra, based on dimensions from the literature. Two models were created, with two different thicknesses of the vertebral body, which were further modified to obtain a mesh structure in the interior of the vertebral body, i.e. a spongy structure.

## 2 BONE PARAMETERS

Bones are made up of bone tissue. This tissue is seen as a composite material, which consists of two phases: an organic phase and an inorganic phase. The former acts as a matrix, while the latter is responsible for reinforcement. The ratio of these phases to each other is 1:2.5. One of the inorganic compounds responsible for mechanical strength is calcium phosphate (V)  $\text{Ca}_3(\text{PO}_4)_2$ , which accounts for 2/3 of the weight of bone. The inorganic components of bone tissue, which make up about 50% of all matrix members, are

responsible for determining bone hardness. The organic phase is formed by bone cells along with the intercellular matrix made up of collagen proteins. They are mainly type I collagen proteins and account for about 95% of all organic components. Collagen found in bone has the ability to resorb calcium, and this distinguishes it from collagen found in other tissues. It is the large amount of collagen in the organic part that changes the elastic properties of bone. The relationship of organic and mineral components determines the mechanical properties of bone [4].

Osteon is the basic structural unit of bone. It is formed by bone lamellae, between which bone cavities are located along with bone cells. In the central part of the osteon is located a central canal called Haversian canal. This is a duct of microscopic dimensions through which blood vessels are routed to allow blood flow to bone cells. Osteons, which are located very close to each other, i.e. one next to the other, result in a compact bone structure (Fig. 1) [3]. Bones by shape are divided into four groups:

- long bone
- short bone
- flat bone
- varus (irregular) bone.

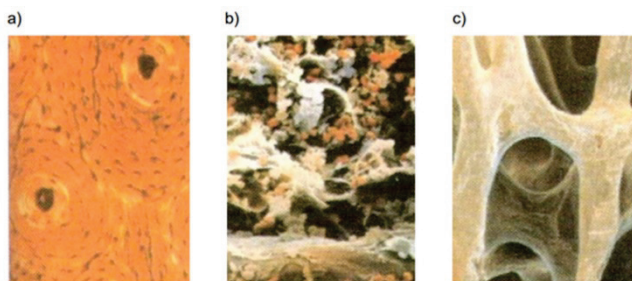


**Figure 1** Bone structure: a) cortical layer - osteons with Haversian canals, b) spongy layer - bone beams, c) bone marrow [5]

Classic long bone consists of bone tissue and marrow. There are two forms of bone tissue: compact bone substance and spongy bone substance. Compact bone tissue is always found on the top layer of the bone so it is called cortical tissue. Through the environment of the bone characterized by an organic substrate, the bone acquires a lot of elasticity. And the calcium salt found there also makes it very resistant to compression and tension. The compressive strength of bone tissue is greater than the tensile strength, while when considering bending, bone is largely less resistant in this aspect [3].

In order to obtain the average values of the mechanical properties of the compact part of the human femur bone, it was examined at appropriate angles, and the obtained values are shown below:

- tensile strength: 107 MPa
- compressive strength: 159 MPa<sup>2</sup>
- torsional strength: 53 MPa
- bending strength: 160 MPa
- ultimate elongation: 135%.

Most of the mechanical properties of bones are due to their anatomical and histological structure. The main concern here is the propensity to fracture, and this is mostly related to

age. Mechanical properties depend on the type of bone structure, geometric form, external loading, location and value of loading forces, which are responsible for the distribution of internal stresses in bones. The collagen content is of great value here, since bones with a high collagen content in their structure are easily subject to brittle fractures. In the case of the elderly, where this collagen in the bones is less and less, brittle fractures occur [4]. The Young's modulus of collagen is 1-2 GPa, and its ultimate tensile strength is 50-1000 MPa [9]. The mechanical properties of spongy bone tissue and compact bone tissue are shown in Tab. 1.

**Table 1** Mechanical properties of two types of bone tissue [6]

Property	Cortical bone	Cancellous bone
Compressive strength (MPa)	100-230	2-12
Flexural, tensile strength (MPa)	50-150	10-20
Strain to failure (%)	1-3	5-7
Fracture toughness (MPa <sup>1/2</sup> )	2-12	-
Young's modulus (GPa)	7-30	0.5-0.05

Spongy bone otherwise known as trabecular bone has a porosity of 50 to 90%, with an average spacing of about 1mm between trabeculae and an average density of about 0.2 g/cm<sup>3</sup>. Compact bone, or cortical bone, has a much denser structure. Its porosity is between 3-12%, and its average density is 1.80 g/cm<sup>3</sup> [6].

### 3 RESEARCH MODELS AND MATERIAL

The structures of the specimen were modeled using Autodesk Inventor Professional 2024. The L2 vertebral body of the lumbar segment was modeled without spinous processes, which are the attachment site of the muscles of the human lower back. In each spinal segment, the vertebrae are different from each other, and this is due to the loads they are subjected to, the mobility they have, and anatomical limitations. The area of the same spinal segment does not contain vertebrae of the same dimensions. Large differences in geometric parameters appear between vertebrae mostly in the vertebral bodies. The vertebral body can be compared to a cylinder having a flat upper and lower surface. However, this does not represent its geometry one hundred percent because the shaft has differences between the size of the upper and lower surfaces, as well as differences in the ratio of the height of the front part to the back part. For the upper part of the shaft, the following parameters were adopted: the width of the upper and lower surfaces of the shaft was assumed to be 51.2 mm, and the depth was 34 mm. The width of the bone ring, which is the outer part of the vertebra, varies according to the analyzed region. The dimensions of the vertebra were taken from the literature entitled Biomechanics of the Spine, by Celina Pezowicz. For the upper part of the bony ring of the L2 vertebra, the width of the area in front was taken into account equal to 5.3 mm, for the sides 6.5 mm, and for the back 3.5 mm - variant A (Fig. 2).

On the other hand, in the lower part of the vertebra, the area of the bone ring in the front is 6.2 mm wide, 8 mm on the sides, and 2.8 mm in the back - variant B (Fig. 3). The dimensions used in the modeling are the average actual

dimensions of the L2 vertebra of an adult in the 36-60 age range.

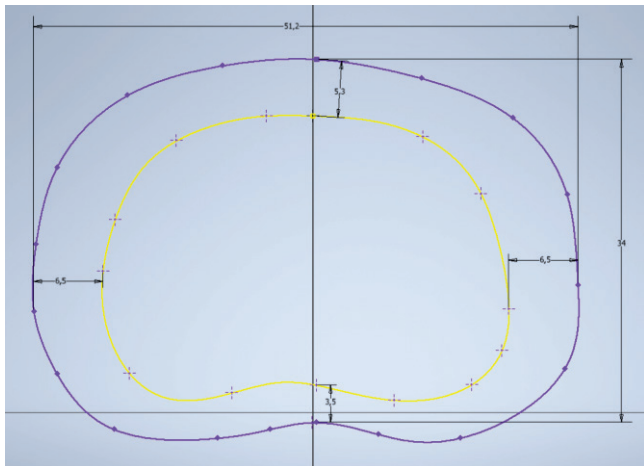


Figure 2 Sketch view with dimensions of the width of the walls of the upper part of the bone ring - variant A

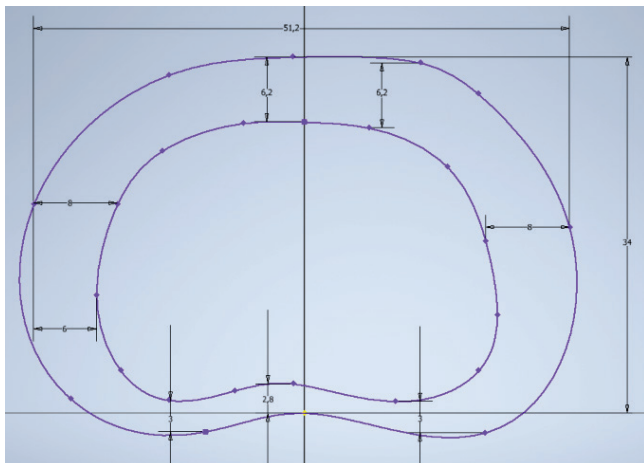


Figure 3 Sketch view with dimensions of the width of the walls of the upper part of the bone ring - variant B

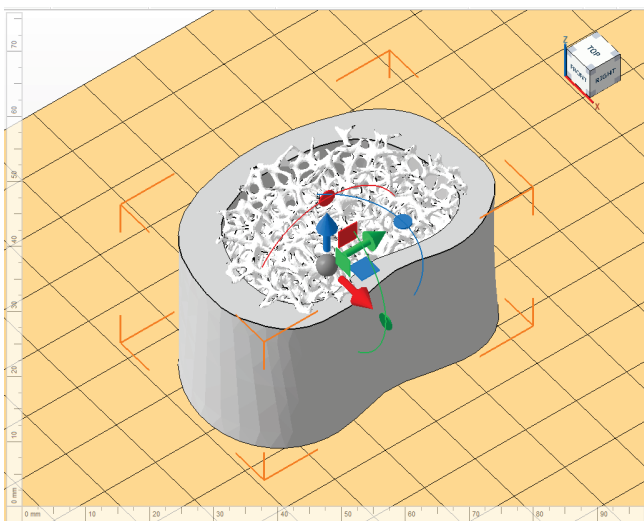


Figure 4 Final model of L2 lumbar vertebra created by Boolean operation from two parts: spongy bone and compact bone in Netfabb software with mesh size 4 x 4 x 4 mm

Netfabb software was used to make the sponge structure inside the compact part. An example of the obtained structure is shown in Fig. 4.

After creating three different models of the L2 lumbar vertebra, research models were made using FFF [10-12] additive technology. Initially, the process had to be prepared and the files were imported into PrusaSlicer. PrusaSlicer is a program for preparing files for 3D printing, which allows the configuration of various printing parameters, such as speed and temperature. The fill of the models was set to 95% due to the fact that often at 100% fill the models do not come out as they should. A grid was used as the fill pattern. No supports were used when printing, and an accuracy of 0.10mm was used in the print settings. The material chosen was PLA, and the printer was Original Prusa i3 MK3S. The test models were made with three densities of the structure mimicking the sponge structure (Fig. 5).

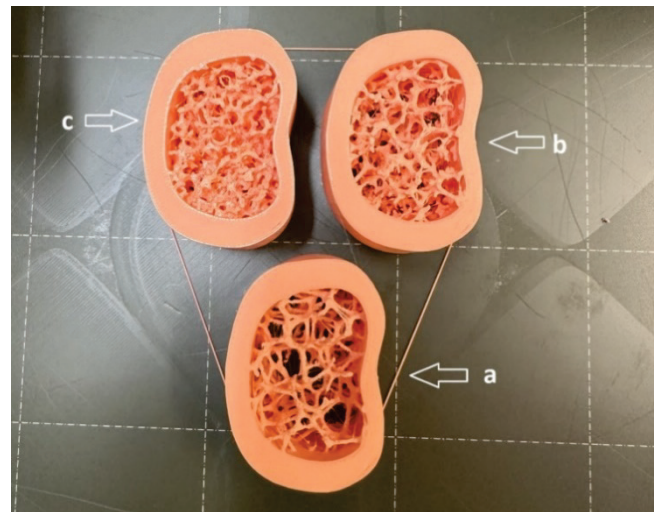


Figure 5 Printed 3D models of the L2 lumbar vertebra with a thicker wall of the vertebral body, with different dimensions of the mesh of the spongy structure: a) 6.5 x 6.5 x 6.5 mm; b) 5 x 5 x 5 mm; c) 4 x 4 x 4 mm

The designations of all research samples are shown in Tab. 2.

Table 2 Designations of research samples

Wall thickness of the vertebra	Density of spongy structure	Designation
Thin wall	6.5 x 6.5 x 6.5 mm	1.1, 1.2, 1.3, 1.4, 1.5
Thin wall	5 x 5 x 5 mm	2.1, 2.2, 2.3, 2.4, 2.5
Thin wall	4 x 4 x 4 mm	3.1, 3.2, 3.2, 3.4, 3.5
Thick wall	6.5 x 6.5 x 6.5 mm	4.1, 4.2, 4.3, 4.4, 4.5
Thick wall	5 x 5 x 5 mm	5.1, 5.2, 5.3, 5.4, 5.5
Thick wall	4 x 4 x 4 mm	6.1, 6.2, 6.3, 6.4, 6.5

The material from which the test samples were made is PLA Polyactide poly(lactic acid) (PLA) is a biodegradable aliphatic thermoplastic polyester, which is a derivative of natural lactic acid. It has a number of unique characteristics that make it an attractive biopolymer in environmental and economic terms, such as excellent rigidity, transparency, ease of processing and aesthetic appearance. Nevertheless, PLA has some limitations, such as intrinsic brittleness, low strength and slower degradation. Nevertheless, it shows great

potential as a biomaterial in various medical fields, including regenerative medicine, orthopedics and tissue engineering [7, 9]. A major advantage of the material chosen for the study is that it can be 3D printed on any device working with FFF additive technology, unlike materials such as PEEK.

PLA is a semi-transparent polymer material that is completely biodegradable by the lactic acid in its structure [12]. However, it decomposes over a fairly long period of time. PLA is not a soluble material. During the printing process, this material does not emit a lot of harmful chemicals, so it can safely be used as an educational aid. The glass transition temperature otherwise softening temperature is about 60 °C. Thanks to its low shrinkage, there is no need to heat the table on which the part is printed from this plastic. The extrusion temperature of PLA filament through the printer's nozzles ranges from 160 to 230 °C. In the case presented, the extrusion temperature was 210 °C. The density of the material between 1.2 and 1.4 g/cm<sup>3</sup>. The material has good tensile strength and stiffness, but limited elasticity and low impact strength. Young's modulus is about 2000 MPa, and yield strength is about 40-50 MPa [1, 13, 14].

#### 4 RESULTS AND DISCUSSION

A static compression test was used to test the printed samples. A motorized force measuring rig of the MultiTest-dV series from Mecmesin was used. The device is used to test forces up to 2.5 kN and elongation of more than 1000%. Since the compression of the sponge part of the printed vertebrae was being attempted, it was necessary to create a punch that was used to compress the selected structure. So, before the compression test of each specimen began, a punch was modeled in AutodeskInventor Professional 2024 (Fig. 6).

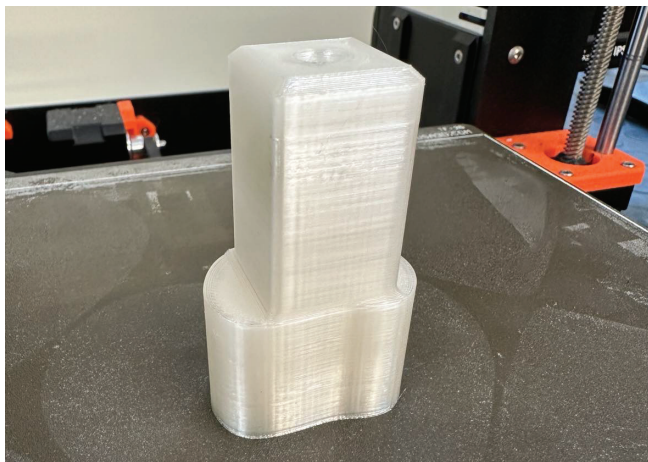


Figure 6 View of a stamp made with FFF 3D printing technology

Fig. 7 shows the specimen after the punch is attached to the machine, and the static compression test process for all printed specimens has begun.

The samples were compressed to a depth of 5 mm, at a rate of 5 mm/min. As an example of the force-time dependence graph, models of a thinner-walled circle with a sponge structure density of 5 × 5 × 5 mm were shown. The

specimens were labeled 2.1, 2.2, 2.3, 2.4, 2.5. The results were tabulated together on a line graph to compare the values obtained (Fig. 8).



Figure 7. Position the sample on the platform under the punch before the compression test

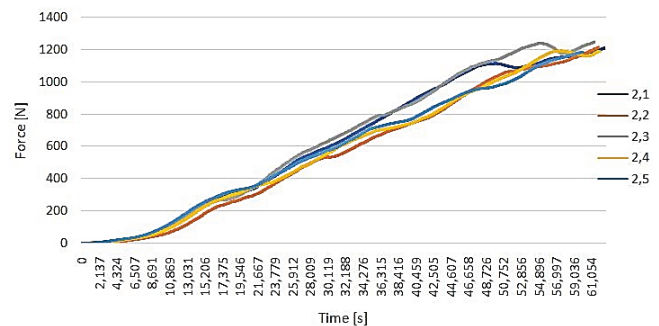


Figure 8 Graph of the force-time dependence of the compression test of thin-walled specimens with a mesh density of 5 × 5 × 5 mm

Spongy tissue is characterized by heterogeneity, and its structure changes depending on its location in the vertebral body. According to the literature, the highest compressive strength values of the spongy tissue of the vertebral body can be observed in its upper and lower parts. During the compression test, the spongy structure was examined to a depth of 5 mm. In order to illustrate what pressure was applied to the specimens during the test and how it varied depending on the particular model, two graphs were created. The first for previously selected representative specimens with thin walls, while the second for representative specimens with thick walls. The strength of the prepared structures was calculated by dividing the highest achieved force in a given compression test by the area on which the force acted.

A graph showing the maximum compressive strength values of the spongy tissue structure in individual specimens with thin and thick vertebral body walls was created from the results of representative samples from each specimen (Figs. 9-10).

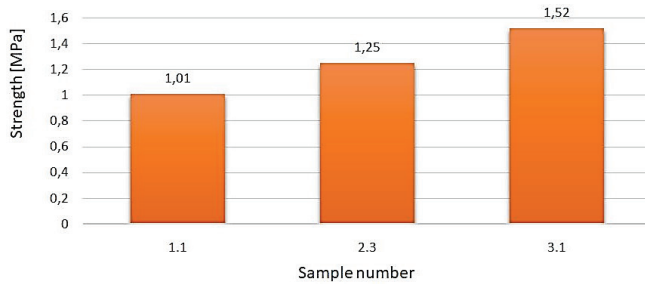


Figure 9. Bar graph showing the maximum compressive strength values of the spongy tissue structure for selected specimens with thin vertebral body walls

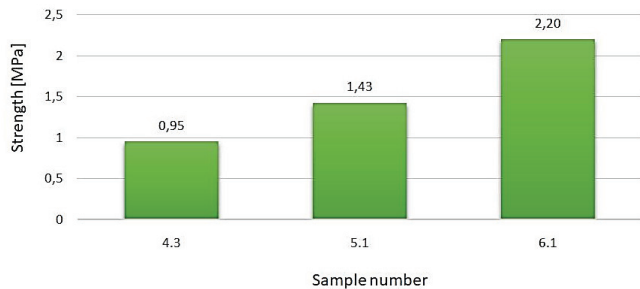


Figure 10. Bar graph showing the maximum compressive strength values of the spongy tissue structure for selected specimens with thick vertebral body walls

According to the literature, the compressive strength of the spongy tissue of the lumbar vertebral bodies ranges from 1.28 to 10.6 MPa [6].

Table 3 Comparison of ranges of maximum compressive strength results of sponge tissue structure for selected specimens with thick and thin vertebral body walls with literature values

	Compressive strength range (MPa)
Literature data	1.28 ÷ 10.6
Samples with thin walls	1.01 ÷ 1.5
Samples with thick walls	0.95 ÷ 2.2

Matching the graph in Fig. 9 showing the values of the maximum compressive strength of the spongy tissue structure for selected specimens with thin vertebral body walls to the literature data yielded groups of specimens that fall within the given range. Of the given groups of specimens with thin walls, only one density of spongy structure met the literature values. Representative sample number 3.1 reached a value above 1.5 MPa, so thin-wall samples with a structure density of  $4 \times 4 \times 4$  mm fall within the specified range. On the other hand, comparing the literature values to those shown in Fig. 10, which shows the values of the maximum compressive strength of the sponge tissue structure for selected samples with thick vertebral body walls, only one group of samples did not reach these values. Samples with the sparsest lattice structure, i.e.  $6.5 \times 6.5 \times 6.5$  mm, where sample number 4.3 was the representative sample, did not even exceed the 1 MPa value. The other two groups, i.e. samples with a mesh density of  $5 \times 5 \times 5$  mm and  $4 \times 4 \times 4$  mm reached values of 1.4 MPa and 2.2 MPa.

## 5 CONCLUSION

The influence of the density of the mesh structure played a major role in the given study. An increase in the density of such a structure, i.e., a decrease in mesh dimensions, led to

an increase in the force that the printed specimens are able to withstand under the assumed parameters, i.e., the maximum compressive force. L2 circle models with a density of  $4 \times 4 \times 4$  mm obtained the highest compressive force values when comparing them to samples with densities of  $5 \times 5 \times 5$  mm and  $6.5 \times 6.5 \times 6.5$  mm.

Specimens with thin walls showed much lower compressive strength than those with thick walls. Regardless of the density of the sponge structure of the L2 vertebral body models. Thicker walls in the specimens improve the absorption and distribution of load during compression tests, which carries with it the obtaining of higher maximum compressive force values compared to specimens with thin walls.

The collapse of the sponge structure and subsequent strengthening of the structure in the case of thin-walled and sparser-textured samples occurred at lower force values. The strengthening of the structure immediately after the collapse is evident when analyzing the resultant graphs of each sample as an increase in force after a previous decrease.

In each group of specimens, the results of the static compression test and the values of the refractive force are very uniform, which indicates good repeatability and homogeneity of the prepared specimens. Slight deviations in the results obtained may be due to small differences in the structure of the material or the conditions under which the tests were performed.

The results obtained show that the proper selection of the density of the sponge structure, as well as the wall thickness, can greatly benefit the mechanical strength of bone implants. The higher the density and the greater the wall thickness, the higher the strength. Which can be important in creating implants with the required properties and strength.

The compressive strength criteria given in the literature for spongy tissue of lumbar vertebral bodies in specimens with thin as well as thick walls are met by a structure with a density of  $4 \times 4 \times 4$  mm. Samples with a mesh density of  $5 \times 5 \times 5$  mm in the case of thick walls also fall within the specified range, but their strength is slightly lower than for samples with a density of  $4 \times 4 \times 4$  mm. The rarest sponge structure, which has a density of  $6.5 \times 6.5 \times 6.5$  mm, does not meet the literature values for compressive strength regardless of wall thickness.

## 6 REFERENCES

- [1] Dave, H. K., Prajapati, A. R., Rajpurohit, S. R., Patadiya, N. H., & Raval, H. K. (2020). Open hole tensile testing of 3D printed parts using in-house fabricated PLA filament. *Rapid Prototyping Journal*, 26(1), 21–31. <https://doi.org/10.1108/RPJ-01-2019-0003>
- [2] Long, J., Gholizadeh, H., Lu, J., Bunt, C., & Seyfoddin, A. (2017). Application of Fused Deposition Modelling (FDM) Method of 3D Printing in Drug Delivery. *Current Pharmaceutical Design*, 23(3), 433–439. <https://doi.org/10.2174/1381612822666161026162707>
- [3] Świczko-Żurek, B. (2009). *Biomateriały*. Gdańsk: Wydawnictwo Politechniki Gdańskiej. (in Polish)
- [4] Pezowicz, C. (2019). *Biomechanika kręgosłupa*. Wrocław: Oficyna Wydawnicza Politechniki Wrocławskiej. (in Polish)
- [5] Smith, J. (1995). *Ciało człowieka*. Warszawa: ZETDEZET.

- [6] Henkel, J., Woodruff, M., Epari, D., et al. (2013). Regeneracja kości w oparciu o koncepcje inżynierii tkankowej — perspektywa XXI wieku. *Bone Research*, 1, 216–248. (in Polish) <https://doi.org/10.4248/BR201303002>
- [7] Wu, W., Geng, P., Li, G., Zhao, D., Zhang, H., & Zhao, J. (2015). Influence of Layer Thickness and Raster Angle on the Mechanical Properties of 3D-Printed PEEK and a Comparative Mechanical Study between PEEK and ABS. *Materials*, 8(9), 5834–5846. <https://doi.org/10.3390/ma8095271>
- [8] Al-Shalawi, F. D., MohamedAriff, A. H., Jung, D.-W., MohdAriffin, M. K. A., Seng Kim, C. L., Brabazon, D., & Al-Osaimi, M. O. (2023). Biomaterials as Implants in the Orthopedic Field for Regenerative Medicine: Metal versus Synthetic Polymers. *Polymers*, 15(12), 2601. <https://doi.org/10.3390/polym15122601>
- [9] Williams, D. F. (Ed.). (1987). *Definitions in biomaterials* (p. 24). Amsterdam-Oxford-New York-Tokyo: Elsevier.
- [10] International Organization for Standardization. (2023). *ISO 17295:2023 Additive manufacturing — General principles — Part positioning, coordinates and orientation*.
- [11] Barrios, J. M., & Romero, P. E. (2019). Decision Tree Methods for Predicting Surface Roughness in Fused Deposition Modeling Parts. *Materials*, 16, 2574. <https://doi.org/10.3390/ma12162574>
- [12] Wohlers Associates. (2024). *Wohlers Report 2024: Analysis. Trends. Forecasts. 3D Printing and Additive Manufacturing State of the Industry*.
- [13] Budzik, G., Magniszewski, M., Przeszlowski, Ł., Oleksy, M., Oliwa, R., & Bernaczek, J. (2021). Torsional strength testing of machine elements manufactured by incremental technology from polymeric materials. *Polimery*, 63(11–12), 830–832. <https://doi.org/10.14314/polimery.2018.11.13>
- [14] Dębski, M., Magniszewski, M., Bernaczek, J., Przeszlowski, Ł., Gontarz, M., & Kielbicki, M. (2013). Influence of torsion on the structure of machine elements made of polymeric materials by 3D printing. *Polimery*, 66(5), 298–304. <https://doi.org/10.14314/polimery.2021.5.3>

**Mariusz Dębski**, Dr  
 Department of Machine Design,  
 Rzeszów University of Technology,  
 al. Powstańców Warszawy 12, 35-959 Rzeszów, Poland  
 +48 17865 1318, m.debski@prz.edu.pl

#### Authors' contacts:

**Lukasz Przeszlowski**, Dr  
 (Corresponding author)  
 Department of Machine Design,  
 Rzeszów University of Technology,  
 al. Powstańców Warszawy 12, 35-959 Rzeszów, Poland  
 +48 17865 1318, lprzeszl@prz.edu.pl

**Anna Paluch**, MSc  
 Rzeszów, Poland

**Grzegorz Budzik**, Prof  
 Department of Machine Design,  
 Rzeszów University of Technology,  
 al. Powstańców Warszawy 12, 35-959 Rzeszów, Poland  
 +48 17865 1318, gbudzik@prz.edu.pl

**Damian Filip**, Dr  
 Department of Orthopedics and Traumatology,  
 University of Rzeszów,  
 al. Tadeusza Rejtana 16C, 35-959 Rzeszów, Poland  
 damian.a.filip@gmail.com

**Lukasz Kochmański**, MSc  
 Department of Machine Design,  
 Rzeszów University of Technology,  
 al. Powstańców Warszawy 12, 35-959 Rzeszów, Poland  
 +48 17865 1318, l.kochmanski@prz.edu.pl